



ELSEVIER

Journal of Chromatography A, 680 (1994) 99–107

JOURNAL OF
CHROMATOGRAPHY A

Microcolumn sample injection by spontaneous fluid displacement

Harvey A. Fishman^a, Richard H. Scheller^b, Richard N. Zare^{a,*}

^a*Department of Chemistry, Stanford University, Stanford,
CA 94305, USA*

^b*Howard Hughes Medical Institute, Department of Molecular and Cellular Physiology, Stanford University, Stanford,
CA 94305, USA*

Abstract

The withdrawal of a capillary structure from a sample solution causes a droplet to be formed at the end of the capillary. Because of the interfacial pressure difference across the curved surface of the droplet, the droplet is driven into the entrance of the capillary, thereby causing injection of the sample. Assuming negligible sample penetration by diffusive or convective mixing, this injection is intrinsically the smallest possible for a capillary. Moreover, the injection volume can be varied by changing the shape of the capillary structure, specifically the outer diameter of the capillary. This injection method eliminates the need for external pressure differences, applied fields across the capillary, or precise timing, thus offering several advantages over conventional procedures. Studies using capillary electrophoresis as the separation procedure show that approximately 3.5 nl (66 μm I.D. capillary) sample volumes can be injected by hand with a reproducibility of $5.8 \pm 0.7\%$ R.S.D. Parameters that affect the variability of the injection are discussed.

1. Introduction

Microchannel separation techniques, such as capillary electrophoresis (CE) and open tubular liquid chromatography, are emerging as powerful methods for analyzing complex mixtures in subnanoliter volumes [1]. In CE, sample can be introduced into the column by either electrokinetic or hydrodynamic injection [2,3]. Electrokinetic injection discriminates among the sample ions based on differences in the electrophoretic mobility and complicates quantitation [4]. Hydrodynamic injection based on pressure differences between the inlet and outlet buffer reservoirs is more reproducible but requires timing

among pressure valves and moving parts [3]. In both methods, a reduction in the injection length improves the separation efficiency but tends to lower the run-to-run reproducibility [5–7].

We describe a method for injection called spontaneous fluid displacement that offers several advantages over conventional injection procedures. Briefly, the injection is based on the formation of a curved meniscus (droplet) at the inlet of a capillary as it is removed from a sample solution [8]. Interfacial pressure differences across the curved surface provide the driving force to inject the sample into the column. In previous work, we identified that this spontaneous injection was largely responsible for the phenomenon called “ubiquitous injection” [8] and offered ways to minimize it. Here, we demonstrate

* Corresponding author.

that spontaneous fluid displacement, previously considered an extraneous injection effect, can itself be used as a reproducible injection method. Because no externally applied pressure or electric field is required for injection, this method may simplify automated injection, and may be useful for a miniaturized CE system or for applications where electric fields or external pressure differences cannot be used. Furthermore, precise timing is unimportant because the entire injection process occurs spontaneously and is complete when the sample has penetrated into the column. This injection method makes possible smaller injection lengths for improvement in separation efficiency in CE [9]. Although the method is applicable to all micro-column separations of liquid samples, we demonstrate its feasibility as an injection method in CE.

2. Theory

The action of removing a capillary from a solution has been shown to result in the attachment of a small droplet and its subsequent spontaneous penetration into the column [8]. By considering the mechanism involved, we can identify parameters that should affect the reproducibility of sample injected into the column. The injection mechanism can be divided into two steps: (a) liquid thread breakup to form the droplet, and (b) droplet penetration into the column by spontaneous fluid displacement (Fig. 1).

2.1. Solution breakup

When the capillary is removed from the sample solution, a thread of liquid spans from the capillary inlet surface to the bulk solution. Eventually, the thread of liquid becomes unstable toward the necking and breaks to form a droplet that adheres to the capillary inlet surface [8]. Rigorous theories to explain mechanisms for solution breakup have been developed for long cylindrical fluid bodies such as liquid jets [10–16] and liquid films supported by fibers (analogous to

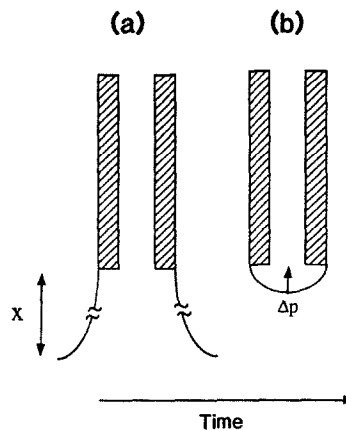


Fig. 1. Schematic depiction of an injection by spontaneous fluid displacement: (a) liquid thread breakup and (b) droplet penetration.

a liquid thread supported by a capillary column) [17]. Because the breakup process of a necking liquid thread supported by a thin fiber shares some of the physical characteristics of that of a liquid jet, considering the more general process of liquid jet instability is useful.

Liquid thread breakup can result from capillary instability [10–17] (Rayleigh instability) or extensional necking [18], and theory describing each phenomenon has been verified experimentally. Moreover, these two breakup processes do not necessarily act independently. For a given set of conditions, the mechanism that causes earlier liquid breakup will determine the droplet volume.

For a cylindrical thread of liquid, small disturbances on the free surface can generate axisymmetric deformations (surface waves) [10]. Because the total surface area is reduced, the resulting liquid structure is thermodynamically more stable than that of a cylinder. The cross-sectional radius, r , of the surface of the thread is then given by [11]

$$r = r_0 + \epsilon \cos \frac{2\pi X}{\lambda} \quad (1)$$

where r_0 is the initial radius of the liquid thread, ϵ is the amplitude of the surface wave of length λ and X is the distance measured along the axis of

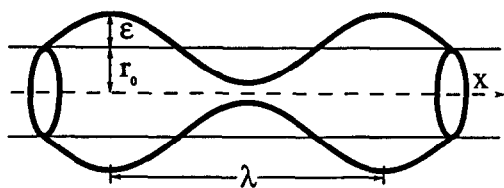


Fig. 2. Schematic illustration of the structure of a liquid jet during breakup by capillary instability. Note the sinusoidal, axisymmetric surface waves.

the thread (Fig. 2). When λ is greater than the circumference of the thread ($2\pi r$), the amplitude of the surface wave grows spontaneously until it equals the radius, r_0 , which causes the thread to pinch off into droplets [10]. Based on this analysis, the drop shapes are determined by a single harmonic waveform [16]. Experiments using stroboscopic photography [16] show, however, that small satellite drops form between the main drops. A refined theoretical model based on a nonlinear analysis can be used to predict this satellite drop behavior [14,16]. As a first approximation though, the amplitude, ϵ , of the wave grows in magnitude according to the expression [11,15]:

$$\epsilon = \epsilon_0 \exp \sigma t \quad (2)$$

where σ is the characteristic growth rate and t is the time. If there are axisymmetric wavelike disturbances of equal amplitude distributed over all wavelengths at the start (white noise), the fastest growing mode (wave) will dominate the breakup and occur at its characteristic growth rate [11,15]. The growth rate for the mode of maximum disturbance has been determined in dimensional form as [15]:

$$\sigma = 0.3433 \cdot \left(\frac{\gamma}{r^3 \rho} \right)^{1/2} \quad (3)$$

where γ is the surface tension, r is the radius of the liquid thread and ρ is the density. The characteristic time for liquid thread breakup is given by $1/\sigma$.

If there is a large enough applied tensile force on the liquid thread, then solution breakup can occur by extensional necking, also called cohe-

sive fracture [18]. During extensional necking, a cohesive fracture results when the applied tensile force exceeds some critical level of stored elastic energy. In the presence of a small tensile force on the liquid, breakup by capillary wave instability does not act independently of this cohesive mechanism; in particular, once the diameter of the thread at the node decreases sufficiently, the liquid cohesively fractures because of the tensile forces acting on it, before it separates into complete droplets.

Presently, the exact mechanism for solution breakup of the thread of liquid supported by a capillary column in this work is unknown. Nevertheless, some conclusions can be drawn from the above discussion. For a given solution, the extensional velocity of removing the capillary from the sample solution favors one mechanism over the other, and may result in a different droplet volume. The extensional velocity, v , can be expressed as:

$$v = \dot{\epsilon} x \quad (4)$$

where $\dot{\epsilon}$ is the extensional rate and x is the maximum distance spanned between the capillary inlet surface and the bulk solution before a cohesive breakup (Fig. 1a). Breakup will most likely occur by capillary instability as long as the capillary is removed from the sample solution at an extensional rate, $\dot{\epsilon}$, slower than the growth rate, σ . For a capillary with 360 μm O.D. and a 20 mM phosphate sample solution, the characteristic time for breakup is approximately 3 ms. As an approximation, breakup is more likely to occur by capillary instability if the extensional velocity of the capillary inlet does not exceed 10 cm/s.

In practice, the actual wavelength that forms on the liquid thread is affected by background noise [11] as well as satellite drop formation [16]. In a typical laboratory, noises (from pump sources or other vibrations) can create surface disturbances at any wavelength and prevent breakup at the mode of maximum instability. To overcome random noise and achieve better wavelength control, audio frequency disturbances can be imposed on the thread and tuned

to the mode of maximum instability [11]. For a liquid jet, when experimental parameters are constant and the amplitude of the applied disturbance is controlled using audio modulations, solution breakup can be made reproducible to better than 10% [11]. In fact, this high level of regularity of droplet formation has been used in ink-jet printing [16].

Still other factors may contribute to droplet formation in liquid structures supported by a fiber (or capillary). For instance, refinements in liquid instability theory that take into account experimental differences between breakup in a liquid jet and breakup in a liquid thread that is supported by a fiber have been developed [17]. Because droplet formation may be affected by any factor that distorts the structure of the liquid thread, reproducibility of this structure is expected to require care. Parameters that may be important include how the capillary is cleaved (because overall surface morphology affects fluid attachment), the wetting properties of the surface surrounding the inlet (which affects the contact angle of fluid attachment), the position and angle of the capillary upon removal, and the radius of curvature of the sample solution into which the capillary is inserted. The precise control of these parameters would therefore be expected to improve reproducibility.

2.2. Spontaneous fluid displacement

Injection of the droplet results from an interfacial pressure difference formed across the curved droplet surface (meniscus) [8]. This pressure difference is large enough to support a $4 \text{ cm} \times 50 \text{ }\mu\text{m}$ column of buffer. If similar droplets are formed, then reproducible injection should occur if the droplet is localized to the tip of the capillary, and sample is not lost from spreading or sticking to the surface or from effects of solvent evaporation [8]. Several key factors that may affect reproducibility of droplet volume and shape include surface tension of the sample solution, surface wettability of the inlet end of the capillary, and vapor pressure surrounding the capillary [8].

The penetration kinetics of the injection are

characterized by an initial high penetration velocity, followed by a leveling off until the droplet has completely entered the column [8]. Allowing the droplet to completely penetrate causes less dependence on precise timing, which should afford high run-to-run reproducibility. For a given capillary structure, penetration kinetics are governed by the surface tension of the sample solution. Thus, two different samples may have slightly different penetration kinetics. In each case, however, equivalent injection volumes will result from waiting until the sample droplet has completely penetrated into the column. More importantly, differences in surface tension between samples will have a greater differentiating effect on losses from surface spreading or from non-uniformities in droplet formation during solution breakage.

3. Experimental

3.1. Chemicals and reagents

All solutions were prepared from a Millipore water-filter system (Milli-Q Plus/UV, Milli-RO 6 Plus; Waters, Bedford, MA, USA). For the CE runs, a 20 mM phosphate buffer, pH 8.7 (Mallinckrodt, San Francisco, CA, USA), was filtered through $0.2\text{-}\mu\text{m}$ pore size syringe filters and used for all studies. Imaging studies were carried out using a 0.4 mM 2',7'-dichlorofluorescein solution (Kodak, Rochester, NY, USA) dissolved in 15 mM, pH 8.9 phosphate buffer. Stock solutions of N^ε-dansyl-L-lysine, N^α-dansyl-L-tryptophan, and dansyl-L-alanine, (Sigma, St. Louis, MO, USA) prepared in the phosphate running buffer were stored in the refrigerator and serially diluted as needed.

3.2. Capillary treatments

The inlet end of a fused-silica capillary column ($52 \text{ }\mu\text{m}$ I.D. \times $131 \text{ }\mu\text{m}$ O.D., $50 \text{ }\mu\text{m}$ I.D. \times $345 \text{ }\mu\text{m}$ O.D., $66 \text{ }\mu\text{m}$ I.D. \times $352 \text{ }\mu\text{m}$ O.D.) (Polymicro Technologies, Phoenix, AZ, USA) was cleaved by first scoring the polyimide coating with a ceramic cleaving square (Polymicro Tech-

nologies) and then carefully bending the capillary to fracture it. With care, this procedure consistently produced a nearly flat surface (as observed under a stereomicroscope) with an angle of $87 \pm 3^\circ$. A 5-mm section of the polyimide coating at the inlet end was removed with a Bunsen burner flame. All capillaries were pre-conditioned with 0.1 M sodium hydroxide (Mallinckrodt), and buffer was then electrophoresed through the column for 1 h. For some studies, the outer surface of the capillary was silanized by holding an air-filled column in a solution of dimethyldichlorosilane in toluene (silanization solution from Supelco, Bellefonte, PA, USA) for 40 min. Afterward, the column was purged with nitrogen and air dried for several minutes. The outer diameter of some capillaries was chemically etched with 0.1 M hydrofluoric acid (Sigma) for 40 min. To maintain a constant inner diameter, the other end of the column was attached to a pressure-regulated nitrogen tank, thereby creating a constant flow of nitrogen through the column to prevent acid from entering the inside of the column. The capillary was rinsed with water before use.

To maintain uniform wetting on the outside surface of the capillary (i.e., to reproduce the surface conditions), excess water-droplet formation on the outside surface was minimized. For the charge-coupled device (CCD) imaging experiments, excess water formation could be reduced by slowly withdrawing the analyte solution from contact with the capillary. Only runs with no noticeable surface spreading after sample contact were used in the CCD imaging studies. Using video imaging of the injection, we found that silanating the outside walls of the capillary inlet helped prevent both excess water drop formation and surface spreading onto the sides upon capillary removal. We silanated the outer walls of the capillary inlet as a preventative measure for the CE experiments.

3.3. CE detection system

Separations were performed using a laboratory-built CE system with an absorbance detector (Isco CV4, Lincoln, NE, USA). The detector wavelength was set at 340 nm with a time

constant of 0.2 s. The voltage control is described elsewhere [19]. The inlet of the capillary was manually transferred from the sample solution (contained in a 1-ml vial) to the inlet reservoir. The capillary was in contact with the sample solution no longer than 5 s. Timing for the transfer was accomplished using either a stopwatch or an alarm timer. During the injection, the sample solution was held approximately 5 mm below the level of the outlet reservoir to prevent inadvertent hydrodynamic injection. Similarly, to prevent loss of the sample from inadvertent hydrodynamic outflow when the capillary was reinserted into the inlet buffer reservoir, we held the outlet reservoir approximately 5 mm below the inlet. A delay of approximately 10 s occurred between reinserting the capillary into the inlet vial and applying the voltage across the capillary. Data were collected with a 486 computer (Adisys, Santa Clara, CA, USA) using Lab Calc data-acquisition software and a Chrom-1AT data acquisition board (Galactics, Salem, NH, USA). Peak areas and heights were determined using Lab Calc.

3.4. Imaging system

Spontaneous fluid displacement injections were quantitated using a fluorescence imaging system described elsewhere [8]. Briefly, the inlet end of a fused-silica capillary column was fixed in position and imaged by a stereomicroscope onto the focal plane of a liquid-nitrogen-cooled (-126°C), scientific-grade CCD camera equipped with a 512×512 CCD chip (PM512, Photometrics).

3.5. CCD image processing

Image dimensions were estimated by using the premeasured outer diameter of the capillary as an internal calibration. Images of the capillaries had similar cross-sectional profiles. From these images we could estimate the position of the edge of the outer capillary wall with an uncertainty of 3 pixels, thus making the absolute internal calibration distances accurate to within 6 pixels (final injection lengths ranged from 50 to

165 pixels). The front end of the capillary was identified by a bright spot that appeared at the front end of all capillaries before and after the fluorescein solution entered the column. The fluorescence response from the channel of the capillary filled with a homogeneous solution of fluorescein was roughly uniform and varied linearly with the concentrations used in these studies.

To determine spontaneous injection lengths, a plot of the fluorescence intensity along the length of the capillary channel was obtained. First, pixels across the width of the channel were averaged. This averaging resulted in a single intensity value for each point along the length of the column, which yields a one-dimensional image slice along the capillary. These slices were converted to one-dimensional text file arrays and then analyzed on a Macintosh IIfx using programs written in Igor (WaveMetrics, Lake Oswego, OR, USA). Plots of the image slice showed the concentration profile along the length of the injection plug. For clarity of presentation, the bright spot present in all of these image slices was removed.

4. Results and discussion

4.1. Injection volume

Spontaneous fluid displacement establishes the feasibility of successively injecting small, fixed volumes in a reproducible manner. A particular capillary inlet has an inherent maximum injection volume that is dependent on its physical characteristics (for, e.g., its morphology, size, etc.). Within this maximum value, the injection volume can be varied in several ways. One method is to reinsert the capillary into the inlet vial at different times during the penetration process, thus placing a larger demand on timing but providing more flexibility for injection. A potentially more reproducible way to vary volume is illustrated in Fig. 3. By changing the outer diameter of the capillary, the amount of droplet formed can be altered.

Fig. 4 shows a comparison of the longitudinal

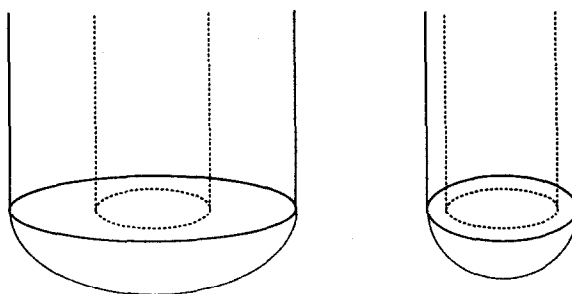


Fig. 3. Schematic diagram of droplet formation at the inlet end of two capillaries with different outer diameters but the same inner diameter.

fluorescence image “slice” of injections from capillaries with different outer diameters but approximately the same inner diameter. The intensity (concentration) profiles along the length of 345 μm O.D. \times 50 μm I.D. and 131 μm O.D. \times 52 μm I.D. capillaries are shown in Fig. 4a and b, respectively. The capillary inlet was surrounded by a saturated vapor atmosphere in both cases. The complete injection for the thin-

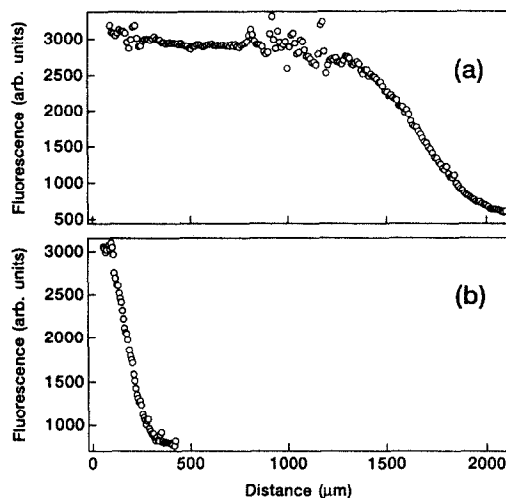


Fig. 4. Fluorescence intensity profiles along the length of an injection by spontaneous fluid displacement. The capillary is surrounded by a vapor-saturated environment. Shown are injections from (a) 50 μm I.D. \times 345 μm O.D. capillary and (b) 52 μm I.D. \times 131 μm O.D. capillary. The sample consisted of 0.4 mM 2',7'-dichlorofluorescein dissolved in 15 mM pH 8.9 phosphate buffer; the column length was ca. 58 cm for each case and was filled with 15 mM pH 8.9 phosphate buffer.

walled capillary occurred within approximately 5 s after the capillary was removed from the sample solution but required approximately 70 s for the thick-walled capillary. As the O.D. of the capillary becomes smaller, so does the radius of curvature of the resulting droplet, which causes the penetration velocity to increase [8]. For a smaller injection, sample entry by diffusive or convective mixing adds a larger component of extraneous injection error [8]. Varying the size between larger-O.D. capillaries is therefore important to minimize error from these mixing processes.

Shown in Fig. 5 are electropherograms that compare spontaneous fluid displacement injection that results from varying the O.D. of a single capillary column (66 μm I.D.). Fig. 5 shows a separation of three dansylated amino acids after a 10-s delay in transfer (between removing the capillary from the sample to inlet

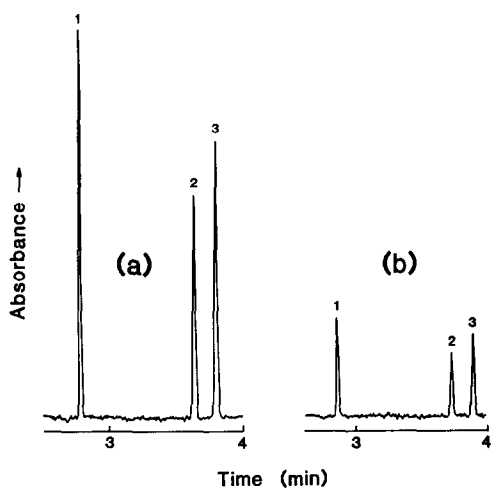


Fig. 5. Electropherograms that demonstrate different injection amounts as a result of varying the outer diameter of a capillary column. Shown are injections from a 66 μm I.D. \times 345 μm O.D. capillary (a) untreated and (b) etched in hydrofluoric acid (0.1 M) for 40 min. The delay time between transferring the capillary inlet from the sample solution and reinserting it into the inlet reservoir was 15 s. The capillary was transferred in an ambient atmosphere. Each electropherogram shows a separation of ca. 0.5 mM each of (1) dansyl-lysine, (2) dansyl-tryptophan and (3) dansyl-alanine. The separation conditions are: capillary length, 60 cm (27 cm to detector); buffer, 20 mM phosphate, pH 8.7; voltage, 20 kV.

reservoir) for an untreated 352 μm O.D. capillary (Fig. 5a), and then for the same capillary whose O.D. was reduced by etching the capillary in hydrofluoric acid for 40 min (Fig. 5b). Although etching the capillary was used here to demonstrate the concept of varying the injection volume by changing the outer diameter, it did not result in a completely uniform annular surface region, and better methods for manipulating the O.D. should be used.

4.2. Reproducibility

Table 1 shows an initial demonstration of the variability for an injection volume of approximately 3.5 nl (66 μm I.D. \times 352 μm O.D. capillary) by spontaneous fluid displacement. Reproducibility in peak areas and peak heights was $5.8 \pm .7\%$ R.S.D. ($n = 11$) for manual injections using a 15-s injection transfer time with the capillary surrounded by an ambient atmosphere. It is difficult to make valid comparisons between different published reports on injection reproducibility because of significant variations in the components and run conditions used. It is useful, however, to mention a range of the best reported values. According to several studies on injection reproducibility [3], variability in peak area ranged from 1–3% R.S.D. for hydrodynamic injection using an automated instrument and from 4–11% R.S.D. using manual injection [7,20]. Moreover, a comparatively higher variability occurred when using electrokinetic injection [3] or when injecting smaller volumes [7,20]. Given that the small injections in this study were performed manually, automated control is expected to significantly reduce the spread. Automated injection would be particularly important for reproducing the extensional necking velocity.

5. Conclusions

We have described an injection method based on spontaneous fluid displacement. Although the injections were made by hand, the reproducibility was approximately $6 \pm 1\%$ R.S.D. Improve-

Table 1
Comparison of peak area and peak height reproducibility for spontaneous fluid displacement injection of three dansylated amino acids

Run	Lys		Trp		Ala	
	Area ^a	Height ^a	Area	Height	Area	Height
1	1.89	103.00	2.11	71.21	2.21	73.00
2	1.87	98.76	2.13	68.45	2.29	76.41
3	1.97	102.99	2.17	70.72	2.28	75.39
4	2.09	112.36	2.29	76.43	2.37	78.27
5	1.91	102.63	2.10	70.79	2.20	73.15
6	1.97	107.06	2.18	74.38	2.30	76.16
7	2.08	111.25	2.29	74.63	2.44	80.39
8	1.73	95.20	1.99	64.81	2.10	70.98
9	1.94	108.57	2.22	71.78	2.26	76.59
10	2.19	115.05	2.42	77.06	2.57	83.54
11	2.17	117.44	2.35	77.72	2.41	80.40
Mean	1.98	106.76	2.20	72.54	2.31	76.75
S.D.	0.138	6.93	0.125	3.94	0.130	3.71
R.S.D. (%)	6.98	6.49	5.66	5.43	5.61	4.83

Lys = Dansylated lysine; Trp = dansylated tryptophan; Ala = dansylated alanine.

^a Arbitrary units.

ments are suggested for lowering the variability. Specifically, we expect that reproducibility will be improved by (1) automating the injection, (2) providing a controlled atmosphere surrounding the capillary entrance, (3) providing a flat, uniform cut at the inlet end of the capillary, (4) isolating the injection process from external vibrations, and (5) preventing the droplet from spreading onto the outside walls of the capillary.

This injection method should be applicable to any microcolumn separation technology and does not require the use of an electric field or application of a pressure difference to the buffer reservoirs. Because some limits exist to the flexibility of injection volumes, this method would be complementary to present forms of injection for more conventional uses of CE. By definition, whenever a capillary is removed from a sample solution into the air, spontaneous fluid displacement represents the smallest injection for a capillary structure (assuming negligible sample penetration by diffusion or convection). Injection by spontaneous fluid displacement could therefore be extremely useful in applica-

tions for which small, reproducible injections are needed, such as calibration and sampling for single-cell analysis. Moreover, for specialized injections, such as sampling human tear film from the eye [21], or for a miniaturized, portable CE system [22,23], injection by spontaneous fluid displacement may be distinctly advantageous over injection by other means.

Acknowledgements

We thank Professor George Homsy, Department of Chemical Engineering, Stanford University, for numerous helpful discussions on the theory of liquid drop formation. We also thank Dr. Shuming Nie, Rajeev Dadoo, and Jason B. Shear for many helpful comments on the manuscript. H.A.F. is a W.R. Grace Foundation fellow. This work was supported by Beckman Instruments, Inc., and the National Institutes of Mental Health (Grant No. NIH 5R01 MH45423-03).

References

- [1] J.W. Jorgenson and K.D. Lukacs, *Science*, 222 (1983) 266.
- [2] S.F.Y. Li, *Capillary Electrophoresis*, Elsevier, London, 1992.
- [3] R. Weinberger, *Practical Capillary Electrophoresis*, Academic Press, Boston, MA, 1993.
- [4] X. Huang, M. Gordon and R.N. Zare, *Anal. Chem.*, 60 (1988) 375.
- [5] H.E. Schwartz, M. Melera and R.G. Brownlee, *J. Chromatogr.*, 480 (1989) 129.
- [6] E.V. Dose and G. Guiochon, *Anal. Chem.*, 64 (1992) 123.
- [7] D.J. Rose, Jr. and J.W. Jorgenson, *Anal. Chem.*, 60 (1988) 642.
- [8] H.A. Fishman, N.M. Amudi, T.T. Lee, R.H. Scheller and R.N. Zare, *Anal. Chem.*, 66 (1994) 2318.
- [9] X. Huang, W.F. Coleman and R.N. Zare, *J. Chromatogr.*, 480 (1989) 95.
- [10] L. Rayleigh, *Proc. London Math. Soc.*, 10 (1878) 4.
- [11] R.J. Donnelly and W. Glaberson, *Proc. Roy. Soc. A*, 290 (1966) 547.
- [12] F.D. Rumscheidt and S.G. Mason, *J. Colloid Sci.*, 17 (1962) 260.
- [13] S.L. Goren, *J. Fluid Mech.*, 12 (1962) 309.
- [14] S.L. Goren, *J. Colloid Sci.*, 19 (1964) 81.
- [15] P.G. Drazin and W.H. Reid, *Hydrodynamic Stability*, Cambridge University Press, Cambridge, 1981, pp. 1–27.
- [16] D.B. Bogoy, *Ann. Rev. Fluid Mech.*, 11 (1979) 207.
- [17] B.J. Carroll and J. Lucassen, *J. Chem. Soc., Faraday Trans. I*, 70 (1974) 1228.
- [18] A. Ziabicki and R. Takserman-Krozer, *Roczniki Chem.*, 37, (1963) 1511.
- [19] J.V. Sweedler, J.B. Shear, H.A. Fishman, R.N. Zare and R.H. Scheller, *Anal. Chem.*, 63 (1991) 496.
- [20] S. Honda, S. Iwase and S. Fujiwara, *J. Chromatogr.*, 404 (1987) 313.
- [21] R. Dadoo, R.N. Zare, S.T. Lin and R.B. Mandell, presented at the 1992 Pittsburgh Conference on Analytical Chemistry and Applied Spectroscopy, New Orleans, LA, 9–12 March 1992, abstract 301.
- [22] D. J. Harrison, K. Fluri, K. Seiler, Z. Fan, C.S. Effenhauser and A. Manz, *Science*, 261 (1993) 895.
- [23] C.S. Effenhauser, A. Manz and H.M. Widmer, *Anal. Chem.*, 65 (1993) 2637.